Journal of Innovative Optical Health Sciences
Vol. 5, No. 3 (2012) 1250019 (10 pages)

DOI: 10.1142/S1793545812500198

ESTABLISHMENT OF VISIBLE ANIMAL METASTASIS MODELS FOR HUMAN NASOPHARYNGEAL CARCINOMA BASED ON A FAR-RED FLUORESCENT PROTEIN

YING ZHENG*, CHUAN HUANG*,
ZHIYONG CHENG† and MIN CHEN*,‡,§
*Britton Chance Center for Biomedical Photonics
Wuhan National Laboratory for Optoelectronics
Huazhong University of Science and Technology
Wuhan 430074, P. R. China
†Wuhan Mechanical Technology College, Wuhan 430075, P. R. China
‡The Hospital of Huazhong University of Science and Technology
Wuhan 430074, P. R. China
§yygybcm@mail.hust.edu.cn

Accepted 21 June 2012
Published 2 August 2012

Background and aims: The spectral properties of enhanced green fluorescent protein (EGFP) used in current visualizable animal models for nasopharyngeal carcinoma (NPC) result in a limited imaging depth. Far-red fluorescent proteins have optimal spectral wavelengths that allow deep tissue penetration, thus are well-suited for the imaging of tumor growth and metastases in live animals. This study aims to establish an imageable animal model of NPC using far-red fluorescent proteins. **Methods:** Eukaryotic expression vectors of far-red fluorescent proteins, mLumin and Katushka S158A, were separately transfected into 5-8F NPC cells, and cell lines stably expressing the far-red fluorescent proteins were obtained. These cells were intraperitoneally or intravenously injected into mice, and their tumorigenic and metastatic potential were examined through fluorescence imaging. Finally, factors affecting their tumorigenic ability were further assessed through testing side population (SP) cells proportion by flow cytometry. **Results:** NPC cell line with high tumorigenicity and metastasis (5-8F-mL2) was screened out, which stably expressed far-red fluorescent protein. Intraperitoneal and intravenous injection of 5-8F-mL2 cells resulted in an abdomen metastasis model and a lung metastasis model. In addition, NPC cell line without tumorigenicity (5-8F-Katushka S158A) was screened out. The percentage of SP cells between 5-8F-mL2 and 5-8F-Katushka S158A was found different, suggesting that the SP cell proportion may play a key role in the determination of cell tumorigenic ability. **Conclusion:** We successfully established animal models for NPC with high tumorigenicity and metastasis using a super-bright far-red fluorescent protein. Owing to the super-brightness and excellent wavelength parameters, these models may be applied as useful tools for intuitive

and efficient monitoring of tumor growth and metastasis, as well as assessing the efficacy of nasopharyngeal cancer drugs.

Keywords: Nasopharyngeal carcinoma; metastasis model; far-red fluorescent protein; fluorescence imaging; side-population cell.

1. Introduction

Nasopharyngeal carcinoma (NPC), also known as "Canton tumor" due to the high incidence in Guangdong, China, is a malignant tumor of the nasopharynx with a strong preference of region and the crowd.[1−5] The occurrence site, which is adjacent with the eyes, ears, nose, throat, base of the skull bone, brain, and other vital organs, is small and hidden, and the symptom often changes, making it difficult for clinical diagnosis.[1,5,6] Thus, it is in an urgent need to establish NPC animal models for the research on detection and treatment of NPC tumors. Traditional animal models for NPC, such as subcutaneous models without any reporter gene, are measureable according to the tumor size, but they cannot be dynamically traced once tumor metastasis occurs in internal tissues and organs.[7,8] Recently, an animal model of NPC based on the enhanced green fluorescent protein (EGFP) was developed,[9−11] which enabled real-time monitoring of growth and development of NPC *in vivo* in subcutaneous models. However, the excitation and emission wavelength of EGFP are 484 and 507 nm, respectively,[12−15] which are far from the near-infrared window, leading to a limited penetration depth in tissue imaging.[16] Therefore, the selection of proper fluorescent protein is essential for the development of NPC animal models.

For a fluorescent protein to be effective for the tissue imaging, it must have optimum wavelength and brightness. Our group has previously obtained a mono-far-red fluorescent protein mLumin[17] (excitation 587 nm, emission 621 nm) via the mutation of S158A based on mKate. The brightness of Katushka S158A was increased by 73% via the mutation of S158A on Katushka (mKate dimer), denoted as Katushka S158A.[18] Based on these studies, we aim to develop animal models for NPC using far-red fluorescent proteins, and expect that those models can be widely used for the dynamic monitoring of tumor growth, metastasis, as well as therapeutic evaluation.

2. Materials and Methods

2.1. *Biomaterials*

Highly metastatic NPC cell line (5-8F) was kindly donated by Dr. Musheng Zeng. BALB/c *nu/nu* mice (SPF) were purchased from the Department of Experimental Animals, Hunan Slack Jingda Laboratory Animal Co., Ltd. Genes of far-red fluorescent proteins (mLumin and Katushka S158A) were constructed by our laboratory.

2.1.1. *Apparatus*

The apparatus used was listed as follows: fluorescent inverted microscope IX-70 (Olympus), FV1000 laser confocal microscope (Olympus), GENios Plus microplate reader (Tecan), homemade small animal whole-body imaging system, FACSVantage flow cytometer (BD), Guava easyCyte 6-2L (Millipore), and CO_2 incubator (Thermo Scientific).

2.1.2. *Reagents*

Reagents included RPMI 1640 cell culture medium (Gibco), fetal bovine serum (FBS, Hyclone), MTS kit (Promega), Verapamil (Sigma), and Hoechst 33342 dye (Amresco).

2.2. *Methods*

2.2.1. *Screening NPC cell lines stably expressing far-red fluorescent proteins*

The far-red fluorescent protein genes were integrated into the eukaryotic expression vector, which were then transfected into 5-8F cells, respectively. By combining limiting dilution and physical removal with toothpicks, the NPC cell lines that stably expressing far-red fluorescent protein (5-8F-mL2 and 5-8F-Katushka S158A) were screened out. The percentage of fluorescent cells in resuspended 5-8F, 5-8F-mL2, and 5-8F-Katushka S158A cells were analyzed by the Guava easyCyte 6-2L system. Then, the

adherent cells were further imaged using a FV1000 laser confocal microscope with a 543 nm laser.

2.2.2. *Evaluation of growth abilities of NPC cell lines stably expressing far-red fluorescent proteins*

5-8F, 5-8F-mL2, and 5-8F-Katushka S158A cells were seeded into 96-well plates (2×10^3/well), with RPMI 1640 containing 10% FBS, and the cell culture medium was replaced with fresh medium every day. The average growth activity of cells in 5 wells was detected each day using a MTS kit (Promega) and this assessment continued for six days. A microplate reader was employed to measure the absorption with a wavelength filter 492/10 nm and a reference wavelength of 620/10 nm.

2.2.3. *Evaluation of* in vivo *tumorigenicity*

All animal studies were complied with the Hubei Provincial Animal Care and Use Committee and the animal experiment guidelines of the Animal Experimentation Ethics Committee of Huazhong University of Science and Technology. Female 4−6 weeks BALB/c *nu/nu* mice were purchased from the Hunan SLAC Jingda Experimental Animals Co., Ltd. 5-8F-mL2 and 5-8F-Katushka S158A cells were treated with trypsin, washed by precooled PBS twice and resuspended at 1×10^7 cells/ml. BALB/c *nu/nu* mice were subjected to intraperitoneal anesthesia with a mixture containing 10% urethane and 2% chloral hydrate. Subsequently, the cell suspension (200 μl, 2×10^6 cells) was hypodermically implanted in the hind leg roots. Thereafter, the tumorigenicity was monitored.

2.2.4. *Establishment of NPC intraperitoneal metastasis model based on the far-red fluorescent protein*

5-8F-mL2 cells (2×10^6) were resuspended in 200 μl PBS after washing twice by precooled PBS. Subsequently, the mixture was intraperitoneally injected into the abdominal cavity of the BALB/c *nu/nu* mice. About 30 days later, the whole-body optical imaging was conducted with excitation wavelength at 562/40 nm, emission wavelength at 655/40 nm and exposure time of 5 s. To subtract the background, imaging was also performed with excitation wavelength at 469/35 nm, emission wavelength at 655/40 nm, and the exposure time of 5 s. Then, the mice were sacrificed by cervical vertebra dislocation. The abdominal cavity was opened and intestine was pulled out for the observation of NPC metastasis. The filter setting were the same as above.[19−24]

2.2.5. *Establishment of NPC tail vein metastasis model based on the far-red fluorescent protein*

5-8F-mL2 cells (2×10^6) were resuspended in 300 μl PBS. The mixture was injected into the nude mice via tail vein injection. About 35 days later, the whole-body optical imaging was performed using the same filter settings described previously with exposure time of 10 s. After the imaging, organs of the mice were dissected for the observation of NPC metastasis through fluorescence imaging with exposure time of 0.4 s.

2.2.6. *Measurement of SP proportion in the cells*

Cells were treated with trypsin, centrifuged, washed with 5 ml PBS twice, and resuspended in precooled medium supplemented with 2% FBS at a final concentration of 1×10^6 cells/ml. The cell suspension was added into sterile EP tubes (1 ml for each tube and two tubes for each cell line). The dyes and drugs were added according to Table 1. The fluorescent dye (Hoechst33342) was added to the tube at a final concentration of 5 μg/ml. Cells were cultured at 37°C for 90 min with interval shaking to prevent the cells from sinking to the bottom and further promote the binding of dyes to the cells. All the EP tubes were placed into the icebox followed by a centrifuge at 1000 rpm, 4°C for 5 min. After the supernatant was discarded, cells were resuspended

Table 1. Pretreatment of 5-8F and 5-8F-mL2 cell lines before FCS measurement.

Dyes and drugs	5-8F	5-8F + verapamil	5-8F-mL2	5-8F-mL2 + verapamil
Verapamil (μM)	0	50	0	50
Hoechst33342 (μg/ml)	5	5	5	5

in 1 ml PBS, and centrifuged again at 1000 rpm, 4°C for 5 min. Finally, cells were resuspended in 200 μl PBS before the flow cytometric analysis. The Hochest33342 blue and Hochest33342 red signals were measured by the FACSVantage flow cytometer (BD), using a 450/55 nm bandpass filter and a 675 nm longpass filter, respectively.[25–27]

3. Results

3.1. *Preparation and characterization of stably far-red fluorescent protein expressing cell lines*

The NPC cell lines that stably expressing mLumin and Katushka S158A were first screened out, which denoted as 5-8F-mL2 and 5-8F-Katushka S158A, respectively. To evaluate their fluorescent properties, flow cytometric analysis and confocal imaging study were performed. As shown in Fig. 1(a), the percentage of fluorescent cells in 5-8F-mL2 and 5-8F-Katushka S158A were 99.8 and 99.5%, respectively. Compared to 5-8F-Katushka S158A cells, 5-8F-mL2 cells showed significant higher fluorescence intensity, which equals to 5−6 times of that of 5-8F-Katushka S158A (Fig. 1(b)). Consistent with the flow cytometric analysis result, confocal imaging showed that almost all 5-8F-mL2 and 5-8F-Katushka S158A cells emitted fluorescence (Fig. 1(c)). When the power of 543 nm laser was 1.5%, the fluorescence intensity of 5-8F-mL2 was saturated. With a lower laser power of 0.5%, the

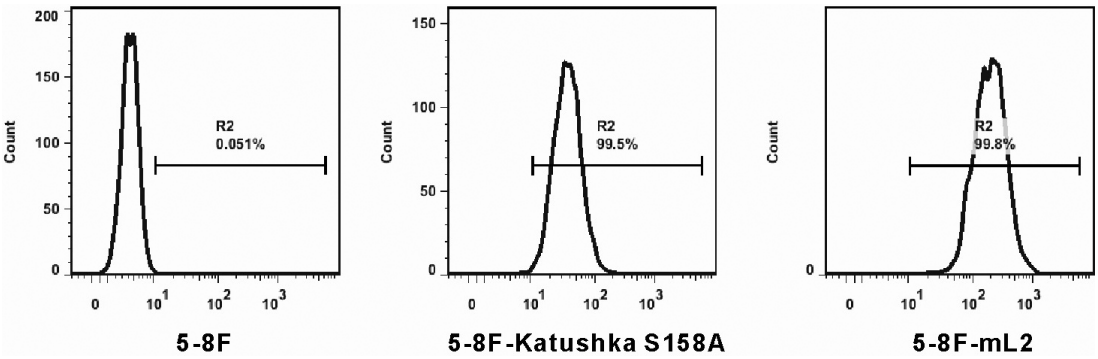

(a)

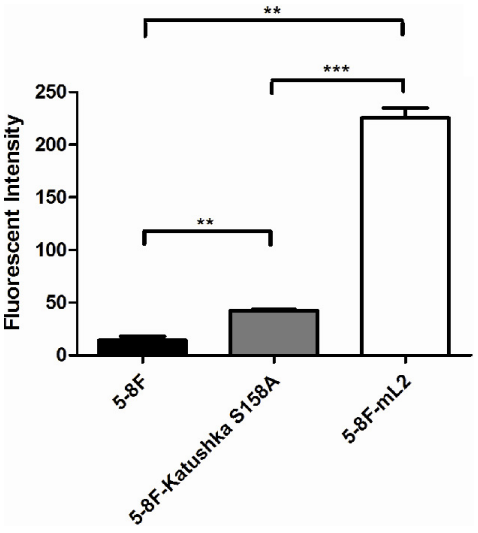

(b)

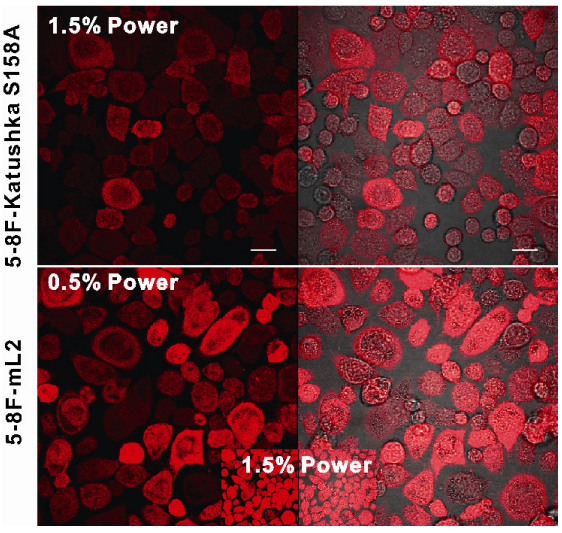

(c)

Fig. 1. Flow cytometry analysis and fluorescent imaging of stable fRFP-expressing human NPC cell lines 5-8F-mL2 and 5-8F-Katushka S158A. (a) and (b) Flow cytometry to quantitative measure the percentage of fluorescence protein-expressing cells, (b) is the quantitative result from (a), $^{**}P < 0.01$, $^{***}P < 0.001$. (c) Fluorescent imaging for the monoclonal cell lines that stably express far-red proteins. Scale bar 20 μm.

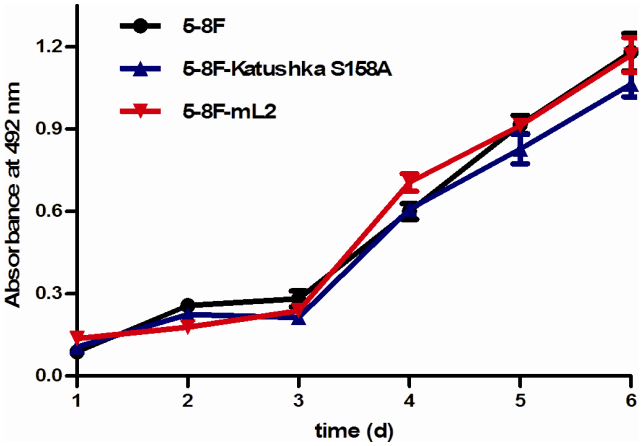

Fig. 2. Comparison of the growth ability of 5-8F, 5-8F-Katushka S158A, and 5-8F-mL2 cell lines *in vitro*. No significant difference is observed between these cell lines (statistics analysis with two-tailed paired *t*-test).

fluorescence intensity of 5-8F-mL2 was similar to that of 5-8F-Katushka S158A under a high laser power of 1.5%. Thus, 5-8F-mL2 cells are more suitable for the following *in vivo* studies than 5-8F-Katushka S158A cells.

3.2. *Growth potential and tumorigenicity of* 5-8F-mL2 *and* 5-8F-*Katushka* S158A *cells*

To investigate whether the integration of fluorescent proteins will affect the growth abilities of NPC, a cell proliferation assay was performed, and these cells were further tested for tumorigenicity in BALB/c *nu/nu* mice through subcutaneous inoculation. As shown in Fig. 2, 5-8F-Katushka S158A and 5-8F-mL2 showed no significant difference with 5-8F, which the corresponding two-tailed *p*-value of 0.0874 and 0.9165, respectively. Additionally, no significant difference was observed between 5-8F-Katushka S158A and 5-8F-mL2 over the studied period, suggesting that the growth potential of 5-8F, 5-8F-Katushka S158A, and 5-8F-mL2 was nearly the same at the cell level. After the inoculation of 5-8F-mL2 cells in BALB/c *nu/nu* mice, a small bulge appeared soon after the inoculation of 5-8F-mL2, which shrank to a minimum size in 3−4 days, and then it started to grow larger steadily and a visible solid tumor formed in seven days post the inoculation, and thereafter the tumor size increased over time. For the mice inoculated with 5-8F-Katushka S158A, a bulge also formed and shrank to a minimum size in 3−4 days. However, no solid tumor was observed during the following 40 days (data not shown). Thus, 5-8F-mL2 cell line was selected for further studies due to its tumorigenic ability.

3.3. *Intraperitoneal metastasis of* 5-8F-mL2 *model for NPC*

Next, we examined the tumorigenic and metastatic ability of 5-8F-mL2 cells through intraperitoneal injection. About 30 days after injection of 5-8F-mL2 cells, results showed that symptoms of abdominal swelling with a hard touch (Fig. 3(a)), abnormal intestinal swelling and liver swelling (Fig. 3(c)) in tumor-bearing mice. In addition, ascites were observed and the small intestine was found abnormally enlarged (Figs. 3(d) and 3(e)). Moreover, the whole body fluorescence imaging was carried out to investigate the location of the metastasis. As shown in Figs. 3(c) and 3(e), there was strong fluorescent signal throughout the abdominal cavity, indicating that 5-8F-mL2 had spread throughout the abdominal cavity. Moreover, the fluorescent signal was mainly distributed in small intestine, large intestine, and mesentery with concomitant multiple metastases, which was further confirmed by the open window imaging, suggesting that an intraperitoneal metastasis model of NPC was successfully established.

3.4. *Lung metastasis of* 5-8F-mL2 *model for NPC*

To establish a NPC model that was different from the intraperitoneal metastasis model, 5-8F-mL2 cells were injected into the BALB/c *nu/nu* mice via tail vein injection. About 35 days later, the whole body fluorescence imaging of nude mice were performed, and subsequently their organs were collected and imaged. As shown in Fig. 4(a), we were able to observe strong fluorescent signal of 5-8F-mL2 cells, which was likely located at the pulmonary region. This was further confirmed by *ex vivo* fluorescent imaging of the excised organs, which showed that the metastasis only occurred in the lung with no detectable signal in other organs, such as the heart, brain, spleen, kidney, liver, and muscle (Fig. 4(c)), suggesting that an imageable lung metastasis model for NPC using 5-8F-mL2 cells was established.

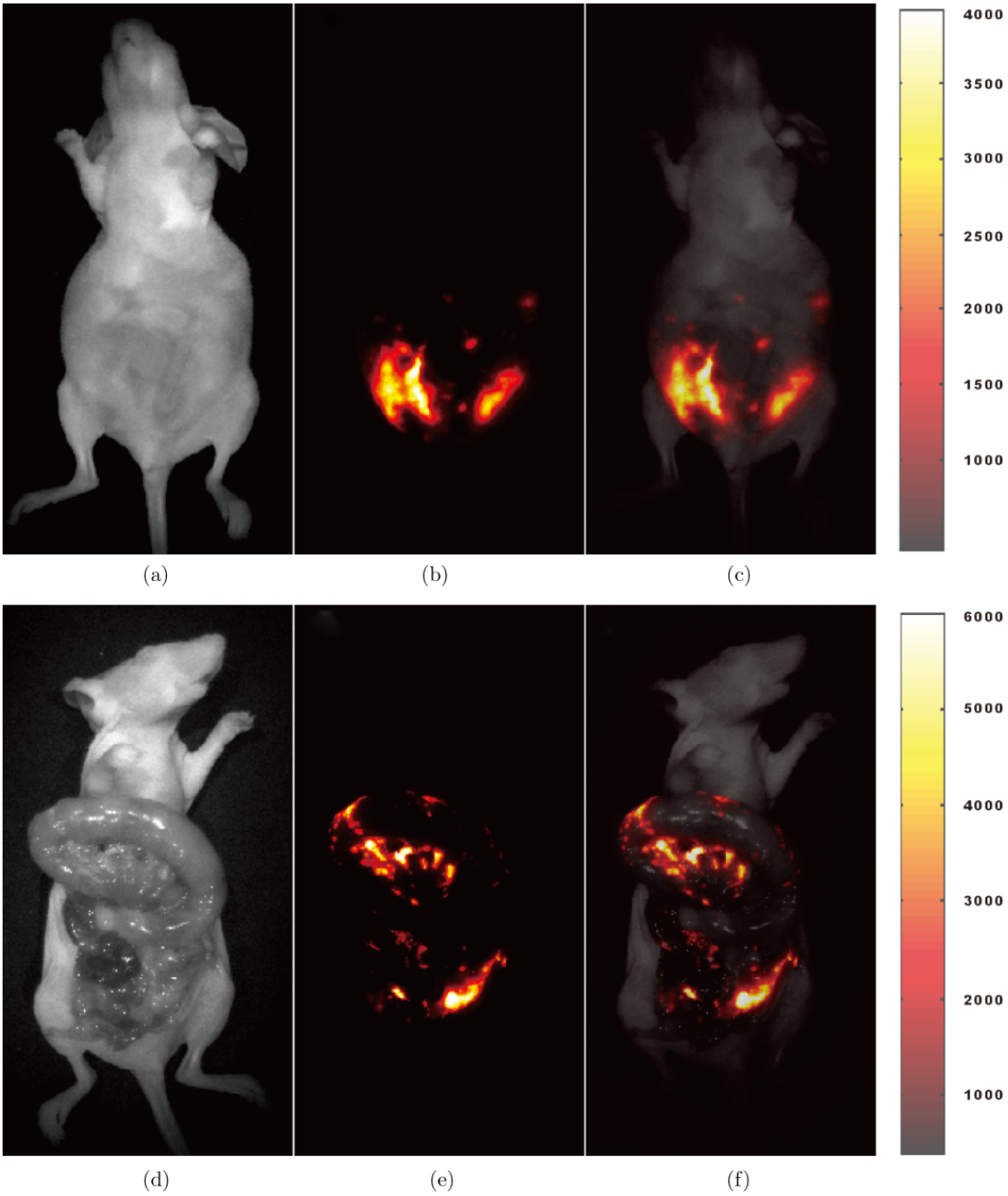

Fig. 3. Representative images of 5-8F-mL2 NPC abdominal cavity metastases model *in vivo*. (a) Bright field, (b) fluorescent, (c) merged images of external whole-body imaging of abdominal cavity metastasis, (d) bright field, (e) fluorescent, and (f) merge images of internal imaging.

3.5. *SP proportion in* 5-8F-mL2 *and* 5-8F-*Katushka* S158A

Since 5-8F-mL2 and 5-8F-Katushka S158A cells are both NPC cell lines expressing far-red fluorescent proteins, and only 5-8F-mL2 cell line shows excellent tumorigenic and metastatic ability, we aimed to investigate the mechanism underlying this difference. We preliminarily analyzed the difference of tumorigenicity by measuring the SP cell content using the initial 5-8F cell line without fluorescence as a control. As shown in Fig. 5(a), the SP cell proportion in 5-8F cells was 4.0% and dropped to

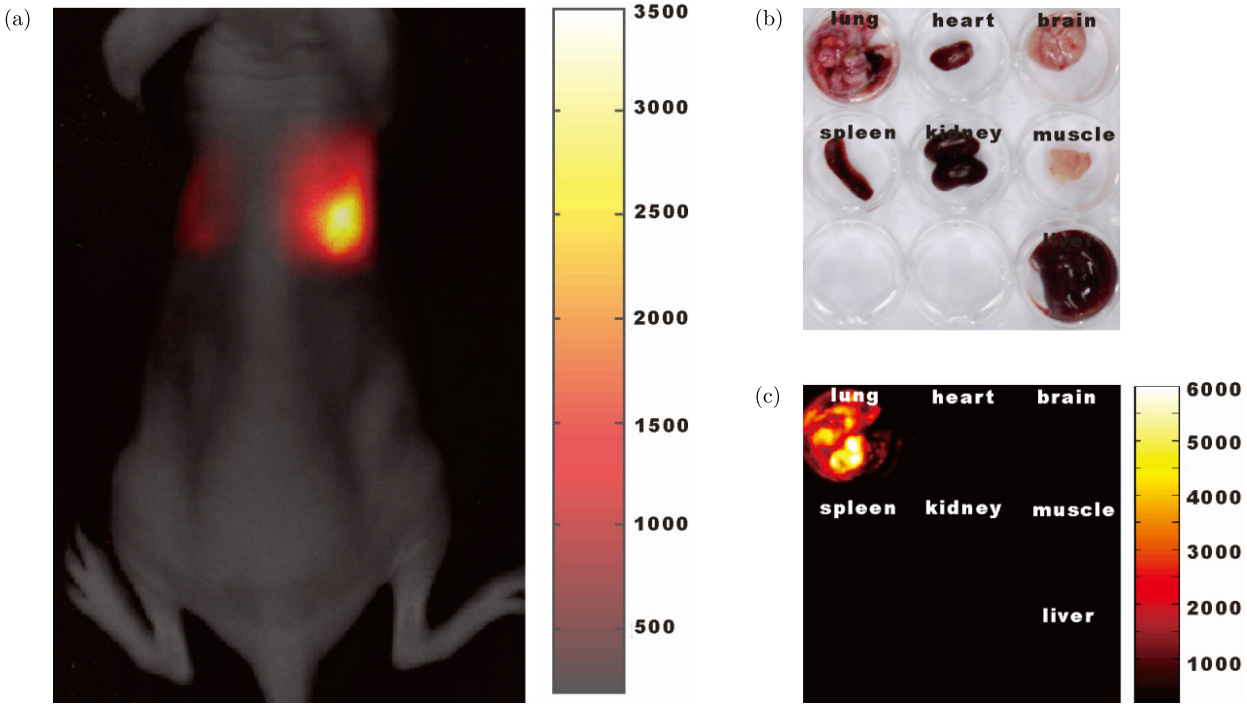

Fig. 4. Representative images of 5-8F-mL2 lung metastases *in vivo* after intravenous injection. (a) Whole-body imaging of lung metastasis, (b) bright field, and (c) representative fluorescent images of organs taken from a sacrificed mouse.

0.2% upon pretreatment with 50 μM ABCG2 (ATP-binding cassette half-transporter member 2 of G family protein) inhibitor Verapamil, which could block the ABCG2 activity to pump extrinsic dyes out of cells,[26] suggesting most of the gated cells were SP cells. Compared with 5-8F cells, the percentage of SP cells in 5-8F-mL2 cells (4.9%) was 1.23 times of that in 5-8F cells (Fig. 5(b)), whereas the proportion of SP cells in 5-8F-KS158A only accounted for 13% of that in 5-8F cells, indicating that the cell tumorigenic ability may be highly correlated with its SP cell proportion.

4. Discussion

In this study, we obtained a NPC cell line (5-8F-mL2) of high tumorigenicity and metastasis that stably express far-red fluorescent proteins, and established the corresponding animal models for subcutaneous tumor and NPC metastasis. In addition, we screened out a NPC cell line (5-8F-Katushka S158A) without tumorigenicity, and found that the SP content may play a role in the determination of tumorigenicity, in which a higher SP proportion corresponds with stronger tumorigenicity.

Previously, the animal model for NPC based on EGFP was developed. However, the spectral properties of EGFP resulted in a high background and limited imaging depth, especially for the observation of the lung and brain metastases, in which only open window imaging can be operated.[11] In compassion, 5-8F-mL2 is a NPC cell line expressing super-bright far-red fluorescent protein. Since mLumin has relatively low absorption by the tissues, long penetration depth in organs and ultra-high expression in 5-8F-mL2 cells,[16–18] we could observe the lung metastasis in the nude mice directly without the open window imaging. The new model provides a useful tool for the real-time monitoring of growth and metastasis of NPC tumor in the BALB/c *nu/nu* mice, and may also be used as a platform for drug screen.

It has been demonstrated that tumor cells often have tumorigenic heterogeneity, showing significant differences in proliferation and tumorigenicity between different cell subtypes. Among these cells, the majority cannot form the tumor or has a limited ability of tumorigenicity, while there is a small portion of cells present which have the capacity of self-renewal, proliferation, and differentiation. This group of cells plays a vital role in the formation and

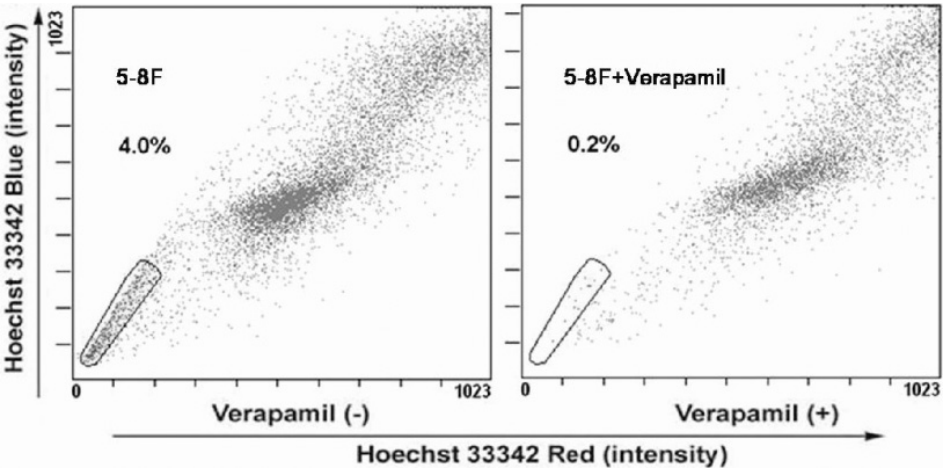

(a)

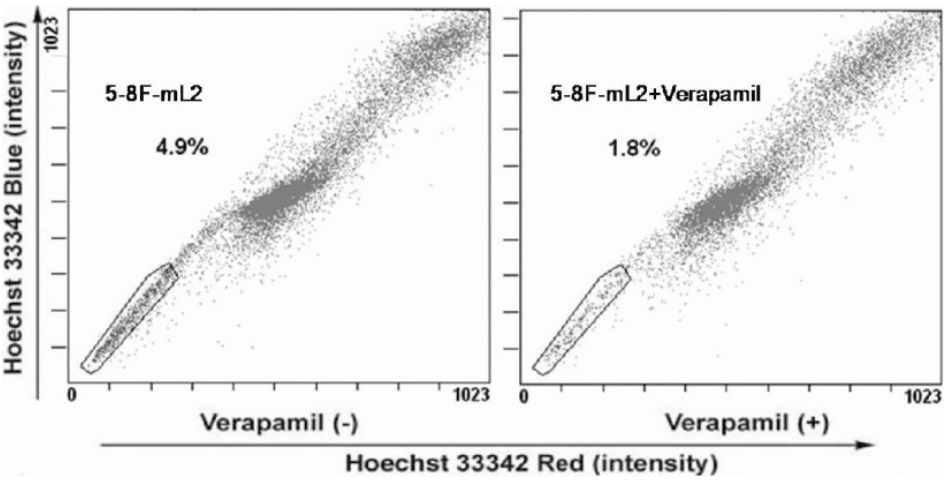

(b)

Fig. 5. SP proportion of 5-8F and 5-8F-mL2 cells measured by using Hoechst 33342. (a) 5-8F cells: The left gate represents the SP cells (4.0% of total cells) and the right gate represents the SP proportion reduced to 0.2% when the cells were pre-incubated with Verapamil to block the ATP transporter. (b) 5-8F-mL2: The left gate represents the SP cells (4.9% of total cells) and the right gate represents the SP proportion reduced to 1.8% when the cells were pre-incubated with Verapamil to block the ABCG2.

growth of tumor, and is denoted as "cancer stem cells".[27–30] SP cell is also called cancer stem-like side population cells, which was discovered when Goodell *et al.* used DNA dye Hoechst 33342 and flow cytometry for the separation of hematopoietic stem cells in 1996.[31] SP cells rely on the dimerization of ABCG2 transmembrane protein that occurs after the binding of ATP. Upon ATP hydrolysis, the conformation changes lead to the transportation of the bonded substrate to the other side of cell membrane with concomitant release of Hoechst 33342 to the extracellular space.[32–34] SP cells have unique phenotypic markers, biological characteristics, and differentiation potential similar to cancer stem cells. In 2007, Zeng *et al.* found that compared to the non-SP cells separated from NPC cells, SP cells has much higher tumorigenic potential and stronger drug resistance.[25] In this work, our results indicated that 5-8F-mL2 cells with high SP proportion exhibit strong tumorigenicity. In contrast, 5-8F-Katushka S158A cells with almost negative SP content do not have any tumorigenic potential. The difference between them is that mLumin is monomer fluorescent protein while Katushka S158A is dimer. However, Katushka S158A itself is not likely to affect the tumorigenesis because there are other tumor cell lines expressing Katushka S158A that maintain the tumorigenicity in our laboratory

(data not shown). Thus, the SP content of tumor cells may be an important factor that requires further consideration prior to the evaluation of *in vivo* tumorigenicity.

In summary, we developed new animal models for NPC based on two NPC cell lines expressing far-red fluorescent proteins. One has the capacity of high tumorigenicity and metastasis, and the other one does not have the tumorigenic ability. These models allow the monitoring of the formation and development of nasopharyngeal carcinoma, and are useful tools for future assessment of efficacy of NPC therapy.

Acknowledgments

The authors thank Prof. Yi-Xin Zeng and Prof. Mu-Sheng Zeng (Sun Yat-sen University Cancer Center, Guangzhou, China) for providing the 5-8F cell line. This work was supported by National Natural Science Foundation of China (Grant No. 81172153) and National Science and Technology Support Program of China (Grant No. 2012BAI23B02).

References

1. A. R. Razak, L. L. Siu, F. F. Liu, E. Ito, B. O'Sullivan, K. Chan, "Nasopharyngeal carcinoma: The next challenges," *Eur. J. Cancer* **46**, 1967 (2010).
2. A. T. Chan, "Nasopharyngeal carcinoma," *Ann. Oncol.* **21**(7), vii308 (2010).
3. A. T. Chan, P. M. Teo, P. J. Johnson, "Nasopharyngeal carcinoma," *Ann. Oncol.* **13**, 1007 (2002).
4. Q. Tao, A. T. Chan, "Nasopharyngeal carcinoma: Molecular pathogenesis and therapeutic developments," *Expert Rev. Mol. Med.* **9**, 1 (2007).
5. L. B. Song, M. S. Zeng, W. T. Liao, L. Zhang, H. Y. Mo, W. L. Liu, J. Y. Shao, Q. L. Wu, M. Z. Li, Y. F. Xia, L. W. Fu, W. L. Huang, G. P. Dimri, V. Band, Y. X. Zeng, "Bmi-1 is a novel molecular marker of nasopharyngeal carcinoma progression and immortalizes primary human nasopharyngeal epithelial cells," *Cancer Res.* **66**, 6225 (2006).
6. X. Li, X. Liu, C. Y. Li, Y. Ding, D. Chau, G. Li, H. F. Kung, M. C. Lin, Y. Peng, "Recombinant adeno-associated virus mediated RNA interference inhibits metastasis of nasopharyngeal cancer cells *in vivo* and *in vitro* by suppression of Epstein−Barr virus encoded LMP-1," *Int. J. Oncol.* **29**, 595 (2006).
7. F. Su, V. Grijalva, K. Navab, E. Ganapathy, D. Meriwether, S. Imaizumi, M. Navab, A. M. Fogelman, S. T. Reddy, R. Farias-Eisner, "HDL mimetics inhibit tumor development in both induced and spontaneous mouse models of colon cancer," *Mol. Cancer Ther.* **11**, 1311 (2012).
8. F. Su, K. R. Kozak, S. Imaizumi, F. Gao, M. W. Amneus, V. Grijalva, C. Ng, A. Wagner, G. Hough, G. Farias-Eisner, G. M. Anantharamaiah, B. J. Van Lenten, M. Navab, A. M. Fogelman, S. T. Reddy, R. Farias-Eisner, "Apolipoprotein A-I (apoA-I) and apoA-I mimetic peptides inhibit tumor development in a mouse model of ovarian cancer," *Proc. Natl. Acad. Sci. USA* **107**, 19997 (2010).
9. T. Liu, W. Xie, L. Liu, K. Yao, "Establishment of visualized cell model 5-8F-EGFP of nasopharyngeal carcinoma," *J. Cancer Control Treat.* **22**, 233 (2009).
10. T. Liu, W. Xie, L. Liu, K. Yao, "Establishment of visualized cell model 6-10B-EGFP of nasopharyngeal carcinoma," *J. Univ. S. Chin.* (*Med. Ed.*) **37**, 393 (2009).
11. T. Liu, Y. Ding, W. Xie, Z. Li, X. Bai, X. Li, W. Fang, C. Ren, S. Wang, R. M. Hoffman, K. Yao, "An imageable metastatic treatment model of nasopharyngeal carcinoma," *Clin. Cancer Res.* **13**, 3960 (2007).
12. A. K. Hadjantonakis, A. Nagy, "The color of mice: In the light of GFP-variant reporters," *Histochem. Cell Biol.* **115**, 49 (2001).
13. B. P. Cormack, R. H. Valdivia, S. Falkow, "FACS-optimized mutants of the green fluorescent protein (GFP)," *GENE* **173**, 33 (1996).
14. S. R. McRae, C. L. Brown, G. R. Bushell, "Rapid purification of EGFP, EYFP, and ECFP with high yield and purity," *Protein Expr. Purif.* **41**, 121 (2005).
15. R. Y. Tsien, "The green fluorescent protein," *Ann. Rev. Biochem.* **67**, 509 (1998).
16. R. Weissleder, V. Ntziachristos, "Shedding light onto live molecular targets," *Nat. Med.* **9**, 123 (2003).
17. J. Chu, Z. Zhang, Y. Zheng, J. Yang, L. Qin, J. Lu, Z. L. Huang, S. Zeng, Q. Luo, "A novel far-red bimolecular fluorescence complementation system that allows for efficient visualization of protein interactions under physiological conditions," *Biosens. Bioelectron.* **25**, 234 (2009).
18. D. Shcherbo, E. M. Merzlyak, T. V. Chepurnykh, A. F. Fradkov, G. V. Ermakova, E. A. Solovieva, K. A. Lukyanov, E. A. Bogdanova, A. G. Zaraisky, S. Lukyanov, D. M. Chudakov, "Bright far-red fluorescent protein for whole-body imaging," *Nat. Methods* **4**, 741 (2007).
19. H. Luo, J. Yang, H. Jin, C. Huang, J. Fu, F. Yang, H. Gong, S. Zeng, Q. Luo, Z. Zhang, "Tetrameric far-red fluorescent protein as a scaffold to assemble an octavalent peptide nanoprobe for enhanced tumor targeting and intracellular uptake *in vivo*," *FASEB J* **25**, 1865 (2011).

20. H. Luo, J. Shi, H. Jin, D. Fan, L. Lu, F. Wang, Z. Zhang, "An (125)I-labeled octavalent peptide fluorescent nanoprobe for tumor-homing imaging *in vivo*," *Biomaterials* **33**, 4843 (2012).
21. R. S. Dacosta, Y. Tang, T. Kalliomaki, R. M. Reilly, R. Weersink, A. R. Elford, N. E. Marcon, B. C. Wilson, "*In vivo* near-infrared fluorescence imaging of human colon adenocarcinoma by specific immunotargeting of a tumor-associated mucin," *J. Innov. Opt. Health Sci.* **2**, 407 (2009).
22. T. Xiong, Z. Zhang, B. F. Liu, S. Zeng, Y. Chen, J. Chu, Q. Luo, "*In vivo* optical imaging of human adenoid cystic carcinoma cell metastasis," *Oral Oncol.* **41**, 709 (2005).
23. J. Fu, X. Yang, G. Quan, H. Gong, "Fluorescence molecular tomography system for *in vivo* tumor imaging in small animals," *Chin. Opt. Lett.* **8**, 1075 (2010).
24. X. Yang, H. Gong, J. Fu, G. Quan, C. Huang, Q. Luo, "Molecular imaging of small animals with fluorescent proteins: From projection to multimodality," *Comput. Med. Imaging Graph* **36**, 259 (2012).
25. J. Wang, L. P. Guo, L. Z. Chen, Y. X. Zeng, S. H. Lu, "Identification of cancer stem cell-like side population cells in human nasopharyngeal carcinoma cell line," *Cancer Res.* **67**, 3716 (2007).
26. L. Yin, P. Castagnino, R. K. Assoian, "ABCG2 expression and side population abundance regulated by a transforming growth factor beta-directed epithelial-mesenchymal transition," *Cancer Res.* **68**, 800 (2008).
27. R. W. Cho, M. F. Clarke, "Recent advances in cancer stem cells," *Curr. Opin. Genet. Dev.* **18**, 48 (2008).
28. L. Patrawala, T. Calhoun, R. Schneider-Broussard, J. Zhou, K. Claypool, D. G. Tang, "Side population is enriched in tumorigenic, stem-like cancer cells, whereas ABCG2+ and ABCG2− cancer cells are similarly tumorigenic," *Cancer Res.* **65**, 6207 (2005).
29. C. G. Marsden, M. J. Wright, R. Pochampally, B. G. Rowan, "Breast tumor-initiating cells isolated from patient core biopsies for study of hormone action," *Meth. Mol. Biol.* **590**, 363 (2009).
30. Y. Liang, Z. Zhong, Y. Huang, W. Deng, J. Cao, G. Tsao, Q. Liu, D. Pei, T. Kang, Y. X. Zeng, "Stem-like cancer cells are inducible by increasing genomic instability in cancer cells," *J. Biol. Chem.* **285**, 4931 (2010).
31. M. A. Goodell, K. Brose, G. Paradis, A. S. Conner, R. C. Mulligan, "Isolation and functional properties of murine hematopoietic stem cells that are replicating *in vivo*," *J. Exp. Med.* **183**, 1797 (1996).
32. X. W. Ding, J. H. Wu, C. P. Jiang, "ABCG2: A potential marker of stem cells and novel target in stem cell and cancer therapy," *Life Sci.* **86**, 631 (2010).
33. C. Hu, H. Li, J. Li, Z. Zhu, S. Yin, X. Hao, M. Yao, S. Zheng, J. Gu, "Analysis of ABCG2 expression and side population identifies intrinsic drug efflux in the HCC cell line MHCC-97L and its modulation by Akt signaling," *Carcinogenesis* **29**, 2289 (2008).
34. H. Zeng, J. W. Park, M. Guo, G. Lin, L. Crandall, T. Compton, X. Wang, X. J. Li, F. P. Chen, R. H. Xu, "Lack of ABCG2 expression and side population properties in human pluripotent stem cells," *Stem Cells* **27**, 2435 (2009).